PCCP

Capillary rise of surfactant solutions†

F. Tiberg,* B. Zhmud, K. Hallstensson and M. von Bahr

Forest Product Section, Institute for Surface Chemistry, Box 5607, S-114 86, Stockholm, Sweden. E-mail: fredrik.tiberg@surfchem.kth.se

Received 5th June 2000, Accepted 17th July 2000
First published as an Advance Article on the web 30th August 2000

The capillary flow of surfactant solutions in hydrophobic and hydrophilic capillaries has been studied. The results obtained are discussed in the light of surface tension relaxation and adsorption phenomena. Modes of surfactant transport and effects of surfactant adsorption, aggregation, and monomer–micelle interconversion on the capillary rise dynamics are further analyzed in the framework of a theoretical model. This provides a self-consistent and quantitatively correct picture of the experimental results. In the case of hydrophobic capillaries, two limiting types of dynamic behavior are adsorption-controlled rise and diffusion-controlled rise. In some cases, slow relaxation of adsorbed layers at the liquid/solid interface can cause a drift of the rise height over a long time under quasi-equilibrium conditions. A slow relaxation, as compared to the capillary rise rate, of the liquid/vapor interface may also produce a maximum in the rise *vs.* time curve. This behavior was, for instance, seen for a surfactant solution penetrating into a hydrophilic capillary.

Introduction

The issue of liquid transport in capillary systems dates back a long time. Basic understanding of the laws of capillarity was gained almost a century ago. Based on the early work by Hagen and Poiseuille,[1–3] Lucas and Washburn[4,5] laid much of the theoretical foundation for describing capillary flow phenomena. This together with some more recent developments[6–14] has been shown to provide a fairly full account of experimental observations for simple liquids.[13–17] However, few fundamental studies have been carried out using complex liquids, for which interfacial tensions and fluid compositions and rheology can change with time due for instance to evaporation of solvent or preferential adsorption of solutes.[14,18–21] In particular, the work by Churaev and Zorin[20] stresses the importance of interfacial adsorption for the penetration dynamics of surfactant solutions. Such studies are necessitated by current technological demands for optimisation of the properties of many technically important and complex systems, including printing inks, paints, coatings, glues, detergent solutions, and various body fluids.

The present investigation is primarily devoted to experimental and theoretical aspects of the capillary rise dynamics exhibited by surfactant solutions in hydrophobic and hydrophilic capillaries. Many of the results obtained are applicable to a broader range of related phenomena, such as surfactant-promoted drop spreading and capillary flow in porous media. The main goal of this study is to clarify the relation between the capillary flow dynamics and interfacial adsorption. For this purpose, a few judiciously chosen model systems are analyzed.

Since the surfactant adsorption is a dynamic process affected by hydrodynamic conditions, mass transport, monomer–micelle conversion rates, and interfacial relaxation processes, the capillary force must be time-dependent. This gives rise to flow characteristics different from those observed for simple liquids. To interpret the observed phenomena it is necessary to consider adsorption at all interfaces, *i.e.* the liquid/solid (ls), the liquid/vapor (lv), and the vapor/solid (vs). Mechanisms of mass-transfer of dissolved surfactants to these interfaces are complex and can involve several sub-processes including bulk diffusion, surface diffusion, and three-phase contact line (tcl) transfer.[12,18,22–25] In most cases, adsorption at the vs interface can be neglected, due basically to the fact that normally there is no surfactant present in the gas phase. Adsorption processes at the lv interface can be followed indirectly by means of various surface tension techniques, while ellipsometry and light reflectometry are essential tools for *in situ* studying adsorption processes at the ls interface.

Experimental details

The experimental setup for studying capillary flow consisted of a glass beaker, which was filled with a surfactant solution to the rim, a glass capillary positioned over the beaker normal to the solution surface, and a video camera connected to a digital video recorder DVCAM DSR-V10P (Sony). The experiment consisted of putting the capillary in contact with the solution and monitoring the z-position of the liquid menicus as a function of time. Fast rise processes were monitored with a high speed Kodak Motion Corder Analyzer SR-1000 camera capable of capturing up to 1000 frames per second. Slower processes were followed with a standard CCD camera. Video data were processed with the NIH Image analysis software (SXM).

The capillaries used in experiments were precision bore borosilicate glass capillaries from Sigma-Aldrich; radii 0.1, 0.15, 0.25 and 0.5 mm. Before measurements, the capillaries were cleaned with bichromate/sulfuric acid solution, rinsed with Millipore water, and dried in a clean air atmosphere at 105 °C. Hydrophobic capillaries were prepared by silylation with dimethyloctylchlorosilane (Fluka, purity >97%) which reacts with the silanol groups present at the surface of glass at room temperature. For silylated surfaces, the advancing and receding contact angles were 110° and 100°, respectively, as

† Presented at the Research Conference on Adsorption to Interfaces, Guildford, UK, April 12–14, 2000.

determined from capillary depression experiments. Prior to use, the hydrophobized capillaries were thoroughly rinsed with tetrahydrofuran and ethanol, and dried at 105 °C.

The surfactants used in this study were high purity hexaethylene glycol monoalkyl ethers, C_nE_6, with decyl ($n = 10$), myristyl ($n = 14$), and palmityl ($n = 16$) chains, purchased from Nikko Chemicals. The critical micellization concentrations (c.m.c.s) of the three surfactants are approximately 1 mM dm^{-3} for $C_{10}E_6$, 0.01 mM dm^{-3} for $C_{14}E_6$, and 0.002 mM dm^{-3} for $C_{16}E_6$, thus differing by three orders of magnitude. Ethoxylated trisiloxane surfactants $[(CH_3)_3SiO]_2Si(CH_3)(CH_2)_2(OCH_2CH_2)_nOH$, also known as M(D′$E_n$)M superspreaders,[26–28] were kindly provided by Dow Corning Corporation.

Results and discussion

The results presented in this section show the principal trends in capillary flow behavior of surfactant solutions. Fig. 1 schematically describes the situation studied. The capillary rise dynamics of surfactant solutions is contrasted to the corresponding behavior of simple liquids. To provide a reasonably broad coverage of the problem, a number of system parameters, including the surfactant chemistry, the bulk concentration of surfactant, and the capillary size, have been deliberately varied and the corresponding effects analyzed.

Major experimental trends

Hydrophobic capillaries. Fig. 2 shows the initial part of the rise height *vs.* time curves measured for a series of $C_{14}E_6$ surfactant solutions in a hydrophobic capillary with the radius of 0.1 mm. It is evident that z scales approximately linearly with t in this time-regime and that the rate of capillary rise is strongly dependent on the surfactant concentration. This regime was apparently overlooked in the earlier study by Churaev and Zorin.[20] Fig. 3 shows the analogous z *vs.* t curves for $C_{10}E_6$ surfactant. The same general tendencies are seen for this surfactant as for $C_{14}E_6$. However, the rise proceeds much faster at similar bulk-concentrations for the $C_{10}E_6$ surfactant and deviations of z *vs.* t plots from linearity are seen after a much shorter time (see Fig. 4). This difference in kinetics can be attributed to a higher c.m.c. of the $C_{10}E_6$ surfactant. This matter will be discussed in more detail later. At this stage, it is worthy of note that this trend is strongly remi-

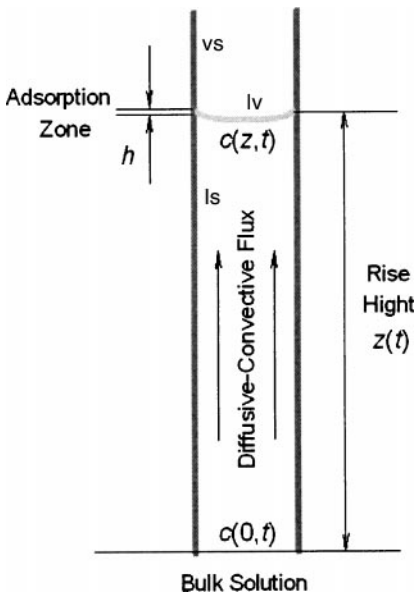

Fig. 1 Schematic representation of the process of capillary rise of surfactant solutions in a hydrophobic capillary.

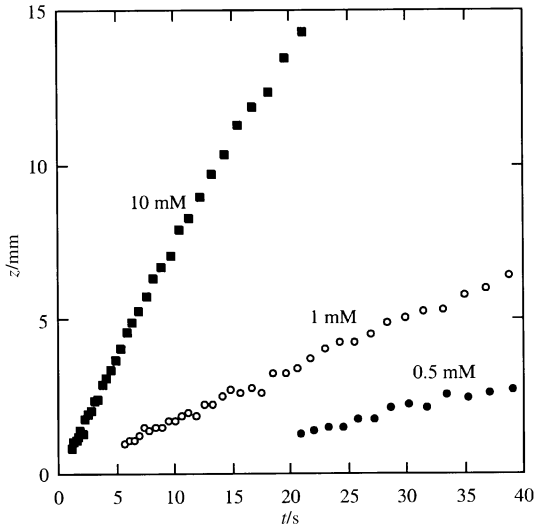

Fig. 2 Short time dynamics of capillary rise observed for $C_{14}E_6$ surfactant solutions with varying bulk concentration (hydrophobic capillary, radius 0.1 mm).

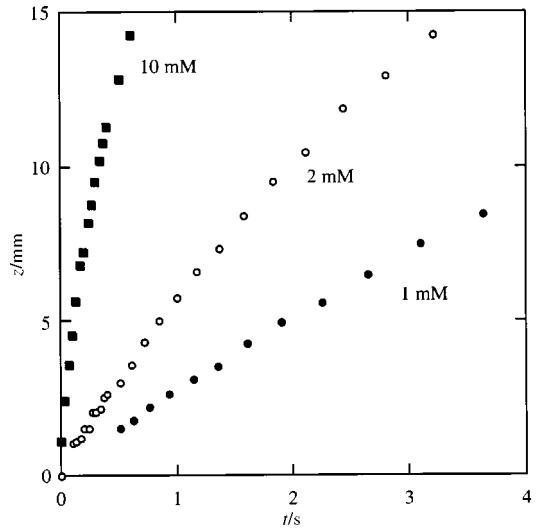

Fig. 3 Short time dynamics of capillary rise observed for $C_{10}E_6$ surfactant solutions with varying bulk concentration (hydrophobic capillary, radius 0.1 mm).

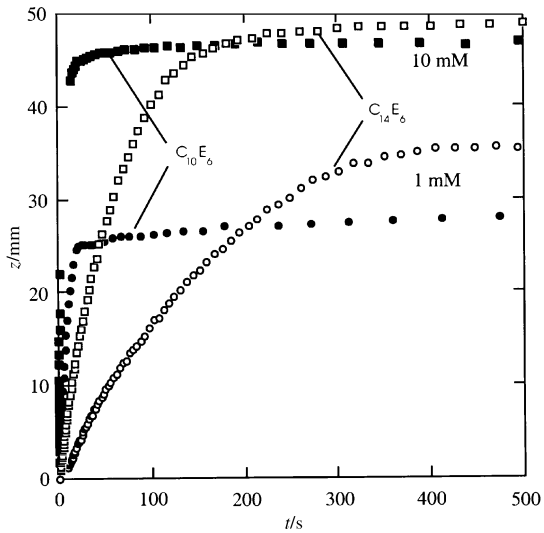

Fig. 4 Capillary rise dynamics observed for $C_{10}E_6$ and $C_{14}E_6$ surfactant solutions at bulk concentrations of 1 and 10 mM in a hydrophobic capillary of 0.1 mm radius.

niscent of the differences in surface tension relaxation dynamics observed for these two surfactants at high concentrations.

As the meniscus moves up in the capillary, surfactant will continuously spill over from the lv to the newly formed ls interface. Unless the loss of surfactant by the lv interface is rapidly compensated by transport from deeper liquid layers, a depletion zone on the top of the liquid column is created and the transport of surfactant becomes the rate-determining stage of capillary rise. Fig. 5 shows the capillary rise dynamics for the same surfactant solutions as in Fig. 2, but followed over a longer period of time and plotted in z *vs.* $t^{1/2}$ coordinates. Clearly, there is a transition in all curves from a linear to a square-root of time regime. Similar results were reported for other surfactant systems.[20]

Fig. 6 shows the influence of the capillary radius on the capillary rise dynamics. The fastest rise is observed in the largest capillary. It is worth noting in Figs. 4, 5 and 6 that, for low surfactant concentration and thin capillaries, the rise stops at a level substantially lower than that one would expect based on the equilibrium surface tension of the corresponding solutions. This reflects the fact that at this height the front zone of capillary column has become depleted of surfactant to a level substantially below the c.m.c. and the diffusion zone has expanded to limits which make the diffusional transport ineffective. That this effect is more pronounced for the thinner capillaries is clearly seen in Fig. 7, where the quasi-equilibrium heights‡ are plotted against concentration for different capillaries. However, after the quasi-equilibrium height has been reached, the build up of the adsorbed layer at the ls interface may not yet be completed. This will lead to a subsequent slow drift towards the equilibrium rise height. Fig. 8 demonstrates this behavior for two solutions of $C_{14}E_6$ surfactant. The slow drift towards equilibrium can be explained by a slow filling of the ls interface to its equilibrium capacity and leveling off of the adsorbate distribution across the interface due to adsorption from the solution and surface diffusion.

If the surface tension relaxation at the lv interface is relatively slow, a maximum at z *vs.* t curves can be observed. Such

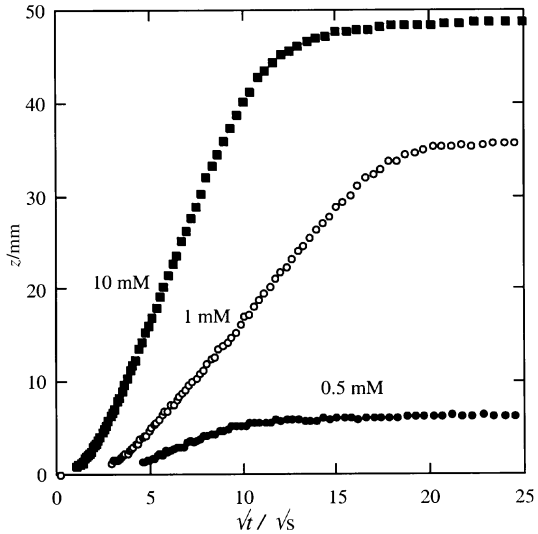

Fig. 5 Capillary rise dynamics observed for $C_{14}E_6$ surfactant solutions (hydrophobic capillary, radius 0.1 mm). Plots of z *vs.* $t^{1/2}$ are partly characteristic of a diffusion-controlled processes.

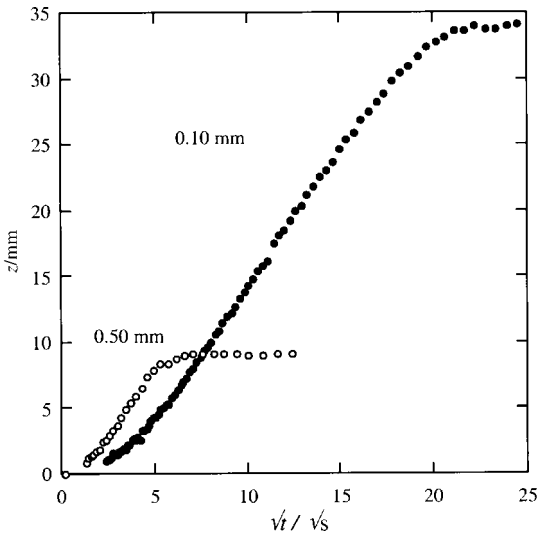

Fig. 6 Capillary rise dynamics observed for 1 mM $C_{14}E_6$ surfactant solutions in hydrophobic capillaries with radii of 0.1 and 0.5 mm.

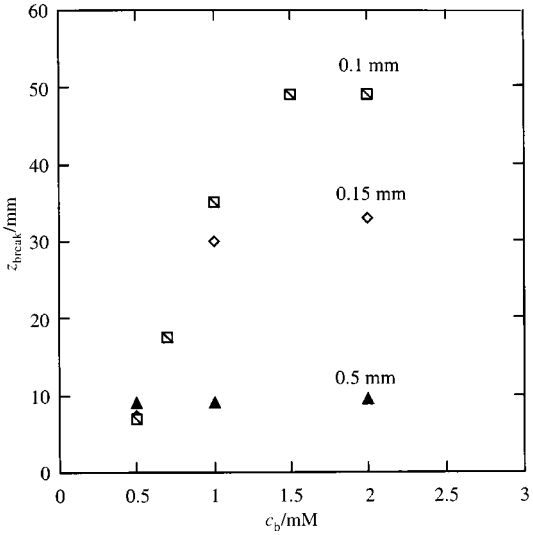

Fig. 7 Dependence of the quasi-equilibrium rise levels on the concentration of surfactant.

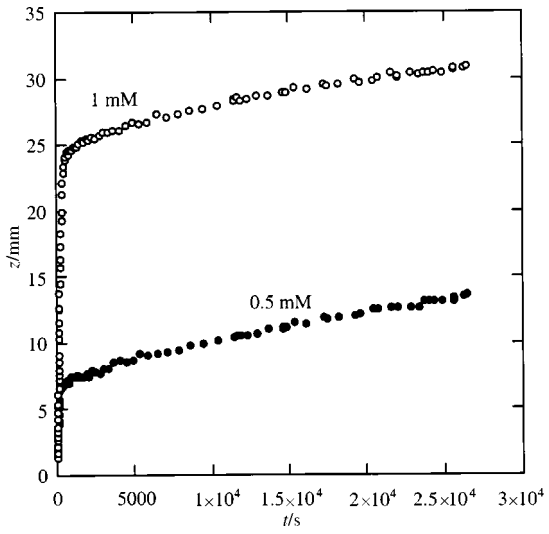

Fig. 8 Long-time capillary rise dynamics observed for $C_{14}E_6$ surfactant solutions in a hydrophobic capillary ($r = 0.15$ mm). A slow drift towards the equilibrium rise height is observed after the quasi-plateau is reached.

‡ Theoretically, the quasi-equilibrium height can be associated with the point of maximum curvature of the z *vs.* t plot. The latter is defined by the conditions $z'' < 0$ (convexity) and $z''' = 0$ (extremum).

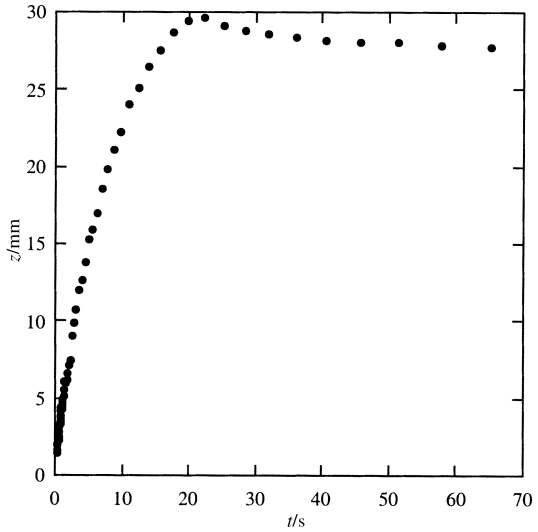

Fig. 9 Capillary rise of a 10 mM aqueous solution of M(D′E_6)M surfactant in a hydrophobic capillary of 0.15 mm radius. An overshoot over the equilibrium height is to be noted.

behavior has been observed when studying the ethoxylated trisiloxane surfactant M(D′E_6)M in methylsilylated hydrophobic capillaries (see Fig. 9). Solutions of this "superspreading" surfactant are slightly opaque[26–28] which indicates the presence of large surfactant aggregates, which diffuse rather slowly and hence limit the transport efficiency to the vs interface.

Hydrophilic capillaries. In contrast to the situation discussed above, water completely wets the inner surface of clean hydrophilic glass capillaries. Therefore, the surfactant adsorption at the ls interface is no longer a factor enabling the rise. The initial stage of the capillary rise dynamics is expected to be similar to that observed for pure water. The capillary flow behavior of surfactant solutions in hydrophilic capillaries will depend on the ratio between the capillary filling time and the surface interfacial relaxation times in a non-trivial way. Fig. 10 illustrates this very nicely for $C_{16}E_6$, which was chosen because it exhibited suitable surface tension relaxation rates for the measurements in question. As can be seen, the capillary rise dynamics in this case depend both on the bulk concentration and the pre-contact condition of the lv interface. When the lv interface is freshly formed immediately before the moment of liquid–capillary contact, a rapid capillary filling is observed. However, the capillary rise height starts to decay after some time, which results in a clear maximum in the *z vs. t* curves. The decay is faster for the 1 mM as compared to the 0.1 mM solution, since the surface tension relaxation is faster for higher surfactant concentrations. Fig. 10 also shows that if the lv interface is allowed to equilibrate prior to the contact with the capillary, the initial rise rate is much slower as compared to the case of a freshly formed interface. This difference reflects an initially lower surface tension of the pre-equilibrated solution. It is also noteworthy that no overshoot in the capillary rise is observed for the pre-equilibrated solution. Evidently, there is no large depletion of the lv interface during the rise in the hydrophilic glass capillary. Fig. 11 shows the short time capillary rise dynamics for pure water as well as for the different surfactant solutions discussed above. All curves show an initial square-root of time dependence of the rise height. For water, this dependence is in agreement with the predications of the Washburn equation, whereas for the surfactant solutions it is related to the time dependence of the lv surface tension (see also below).

Another way of observing the overshoot was by quenching the solution below the Krafft temperature before contact with the capillary. This slowed down the lv tension relaxation rate

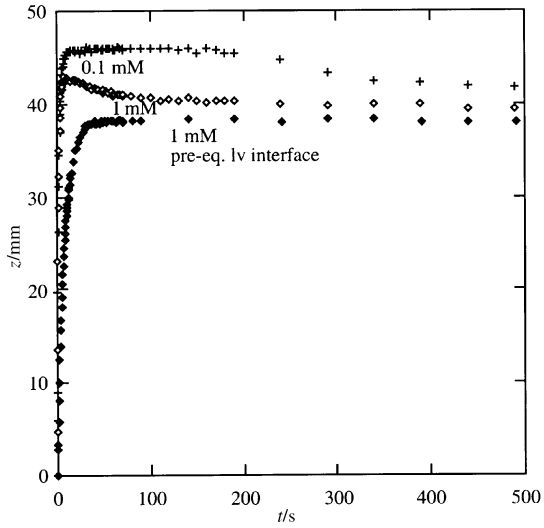

Fig. 10 Capillary rise of 0.1 mM and 1 mM aqueous solutions of $C_{16}E_6$ surfactant in a clean hydrophilic (non-modified) glass capillary of 0.15 mm radius. An overshoot over the equilibrium height is to be noted in the cases where the lv interface was not allowed to equilibrate before contact between the capillary and the solution. For the solution with the pre-equilibrated interface, a monotonous rise to a steady-state height was observed.

sufficiently for the overshoot to be observed for the 1 mM solution with the pre-equilibrated lv interface (see Fig. 12).

Theoretical interpretation

Adsorption at the liquid/solid interface. The head zone is enriched by surfactant due to its adsorption to the lv interface (see Fig. 1). For typical surfactant adsorption values, the concentration of surfactant in the adsorption zone is many orders of magnitude higher than in the bulk. The thickness of the adsorption zone can be defined by

$$h = \frac{\int_{-\infty}^{+\infty} [\exp(-\beta\Phi(z)) - 1]\, dz}{\exp(-\beta\Phi_{min}) - 1}, \quad \beta = (kT)^{-1} \qquad (1)$$

where Φ is the adsorption potential; negative values of Φ corresponds to positive adsorption, and Φ_{min} represents the depth of the potential well. The numerator in eqn. (1) defines the net surface excess, while the denominator gives the maximum

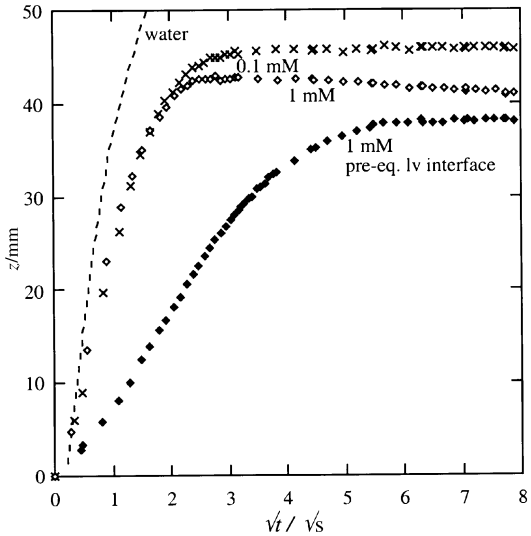

Fig. 11 Short-time dynamics of the capillary rise of 0.1 mM and 1 mM aqueous solutions of $C_{16}E_6$ surfactant in a clean hydrophilic (non-modified) glass capillary (see Fig. 10 for details). For comparison, the capillary rise dynamics of pure water are also plotted.

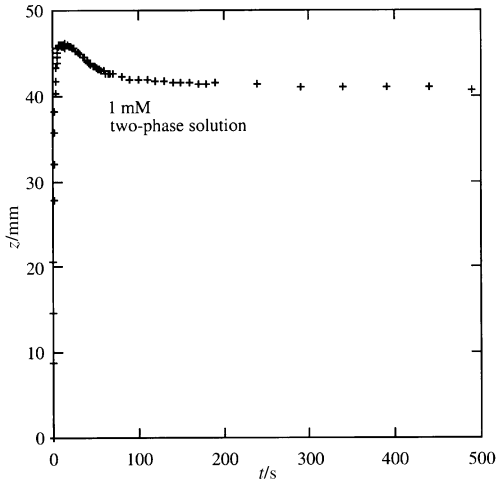

Fig. 12 Dynamics of the capillary rise of a 1 mM aqueous solutions of $C_{16}E_6$ surfactant in a clean hydrophilic (non-modified) glass capillary. The solution temperature has been quenched below the Krafft temperature to slow down the surface relaxation process. The lv interface was allowed to equilibrate before contact with the capillary.

density of adsorbate in the adsorbed layer. Typically, h has the order of magnitude of a few molecular diameters, *i.e.* is negligible as compared to the system dimensions. For that reason, it is a reasonable assumption that surfactant spills from the liquid/vapor interface on the liquid/solid interface as the liquid meniscus is advancing upwards. This has also been supported by recent ellipsometric studies,[29] in which the ls adsorption near the tcl has been studied during immersion of the substrate into surfactant solutions. Since the adsorbed layer at the lv interface is a mobile one, there should not be any significant pressure gradients over the layer and the adsorption should be homogeneous.

Let the adsorption follow the Langmuir–Hinshelwood kinetic equation,

$$\frac{\mathrm{d}\Gamma_{\mathrm{ls}}}{\mathrm{d}t} = \frac{k_{\mathrm{ls}}^{+}\,\Gamma_{\mathrm{lv}}}{h}\left(1 - \frac{\Gamma_{\mathrm{ls}}}{\Gamma_{\mathrm{ls}}^{\mathrm{m}}}\right) - k_{\mathrm{ls}}^{-}\,\frac{\Gamma_{\mathrm{ls}}}{\Gamma_{\mathrm{ls}}^{\mathrm{m}}} \tag{2}$$

where Γ_{ls} is the amount of surfactant adsorbed to ls interface from the lv interface near the triple phase contact line, $\Gamma_{\mathrm{ls}}^{\mathrm{m}}$ is the monolayer capacity for the ls interface, h is the thickness of the adsorption layer, and k_{ls}^{+} and k_{ls}^{-} are, respectively, the adsorption and desorption rate constants. Since surfactants are strongly adsorbed, *i.e.* typically $K_{\mathrm{ls}}^{+}\,\Gamma_{\mathrm{lv}}/hk_{\mathrm{ls}}^{-} \gg 1$, the following approximate solution can be used,

$$\Gamma_{\mathrm{ls}} = \Gamma_{\mathrm{ls}}^{\mathrm{m}}\left\{1 - \exp\left(-\frac{k_{\mathrm{ls}}^{+}}{h\Gamma_{\mathrm{ls}}^{\mathrm{m}}}\int_0^t \Gamma_{\mathrm{lv}}\,\mathrm{d}t\right)\right\} \tag{3}$$

If the liquid front moves with a velocity $v = z'$ (here $' = \mathrm{d}/\mathrm{d}t$), each area at the ls interface spends on average a time h/z' in contact with the surfactant-rich surface layer. If Γ_{lv} does not change significantly over this time, a further simplification is justified,

$$\Gamma_{\mathrm{ls}} = \Gamma_{\mathrm{ls}}^{\mathrm{m}}\left\{1 - \exp\left(-\frac{k_{\mathrm{ls}}^{+}\,\Gamma_{\mathrm{lv}}}{\Gamma_{\mathrm{ls}}^{\mathrm{m}}\,z'}\right)\right\} \tag{4}$$

Since the lv interface is continuously depleted by transfer of surfactant to the ls interface, a diffusional flux will develop bringing surfactant along the liquid column from deeper zones to the top. This is schematically depicted in Fig. 1.

Dynamics of capillary flow. In contrast to pure liquids, where the capillary force is essentially a constant, in surfactant solutions the latter is allowed to change as the meniscus is advancing through the capillary. To extend the analogy with pure liquids, $f(t)$ can be factorized as

$$f(t) = \gamma_{\mathrm{lv}}(t)\cos\,\theta(t) \tag{5}$$

where γ_{lv} is the dynamic surface tension of the lv interface, and θ is the dynamic contact angle. It should be noted that any change in contact angle involves a change in the area of the lv interface and a redistribution of mass. However, the related flow pattern effects near the capillary entrance are neglected here.

Initially the capillary surface is assumed to be absolutely non-wettable, *i.e.* the initial value of the contact angle is 180°. Then, from the balance of tensions acting at the triple contact line, it follows that in this initial state

$$\gamma_{\mathrm{ls}}^{180} = \gamma_{\mathrm{lv}} + \gamma_{\mathrm{vs}} \tag{6}$$

(the subscript vs refers to the vapour/solid interface). Adsorption of surfactant to the ls interface reduces its surface tension, thereby enhancing its wettability. If the final state is a completely wettable surface, the contact angle reduces to zero, and

$$\gamma_{\mathrm{ls}}^{0} = -\gamma_{\mathrm{lv}} + \gamma_{\mathrm{vs}} \tag{7}$$

An exact link between the γ_{ls} and the amount of surfactant adsorbed is established by the Gibbs equation. For our purposes, a simplified linear relation will suffice,

$$\begin{aligned}\gamma_{\mathrm{ls}} &= \gamma_{\mathrm{ls}}^{180} - [\gamma_{\mathrm{ls}}^{180} - \gamma_{\mathrm{ls}}^{0}]\,\frac{\Gamma_{\mathrm{ls}}}{\Gamma_{\mathrm{ls}}^{\mathrm{m}}} \\ &= \gamma_{\mathrm{ls}}^{0} + [\gamma_{\mathrm{ls}}^{180} - \gamma_{\mathrm{ls}}^{0}]\exp\left(-\frac{k_{\mathrm{ls}}^{+}}{h\Gamma_{\mathrm{ls}}^{\mathrm{m}}}\int \Gamma_{\mathrm{lv}}\,\mathrm{d}t\right)\end{aligned} \tag{8}$$

Consequently, the capillary force can be written as

$$f(t) = \gamma_{\mathrm{lv}}(t)\left[1 - 2\,\exp\left(-\frac{k_{\mathrm{ls}}^{+}}{h\Gamma_{\mathrm{ls}}^{\mathrm{m}}}\int_{t(z-h/2)}^{t(z+h/2)} \Gamma_{\mathrm{lv}}\,\mathrm{d}t\right)\right] \tag{9}$$

After the capillary has been put in contact with a surfactant solution, the liquid will not enter it until a positive capillary force, $f(t) > 0$, builds up. Hence, an initial delay should be expected. Furthermore, as long as $z \approx 0$ and the concentration of surfactant in the bulk solution is equalized by forced convection, the adsorption at the lv interface has to be close to its equilibrium value, $\Gamma_{\mathrm{lv}} \approx \Gamma_{\mathrm{lv}}^{\mathrm{eq}}$ (the latter can be evaluated from DST titration data). Therefore, based on eqn. (9), the delay time can be estimated as

$$\tau = \frac{h\Gamma_{\mathrm{ls}}^{\mathrm{m}}\,\ln\,2}{k_{\mathrm{ls}}^{+}\,\Gamma_{\mathrm{lv}}^{\mathrm{eq}}} \tag{10}$$

in a sense that $f(t) = 0$ as $t = \tau$. Thus, if time is counted from the moment that the capillary touches the solution, no rise is observed in the interval $0 < t < \tau$. Moreover, if the capillary is dipped into solution, an initial depression should, rather, be observed. At $t = \tau$, the capillary force changes its sign. In another instant, $t = \tau + \delta t$, the force is incremented by

$$\delta f = \gamma_{\mathrm{lv}}\,\frac{k_{\mathrm{ls}}^{+}\,\Gamma_{\mathrm{lv}}^{\mathrm{eq}}}{h\Gamma_{\mathrm{ls}}^{\mathrm{m}}}\,\delta t \tag{11}$$

and $\delta f \to 0$ as $\delta t \to 0$. Therefore, in this limit, all terms in the equation of dynamics appear to be negligible, so that the adsorption, or better to say, the gradient of the chemical potential, remains the only factor that drives the solution up. The velocity of the liquid front at $z = 0$ can be estimated from the mass balance,

$$2\pi r\Gamma_{\mathrm{ls}}^{\mathrm{m}}\,\mathrm{d}z = \pi r^2\left(\frac{k_{\mathrm{ls}}^{+}\,\Gamma_{\mathrm{lv}}^{\mathrm{eq}}}{h} - D\,\frac{\partial c}{\partial z}\bigg|_{z=0}\right)\mathrm{d}t \tag{12}$$

where D is the diffusion coefficient of surfactant molecules. Since the rise is infinitesimal while D is finite, no depletion of the lv interface is possible,

$$\frac{\mathrm{d}\Gamma_{\mathrm{lv}}}{\mathrm{d}t} = -\frac{k_{\mathrm{ls}}^{+}\,\Gamma_{\mathrm{lv}}^{\mathrm{eq}}}{h} - D\,\frac{\partial c}{\partial z}\bigg|_{z=0} = 0 \tag{13}$$

hence,

$$\left.\frac{\partial c}{\partial z}\right|_{z=0} = -\frac{k_{ls}^{+}\,\Gamma_{lv}^{eq}}{hD} \tag{14}$$

On substituting this result into eqn. (12), the initial velocity of the liquid front is found,

$$v_0 \equiv \left.\frac{\mathrm{d}z}{\mathrm{d}t}\right|_{z=0} = \frac{rk_{ls}^{+}\,\Gamma_{lv}^{eq}}{h\Gamma_{ls}^{m}} \tag{15}$$

This behavior is different from the behavior of liquids in hydrophilic capillaries. Thus, the Lucas–Washburn equation predicts a burst-like dynamics with the velocity being infinite at the beginning. Taking into account the inertia effects eliminates this drawback of the Lucas–Washburn theory, leading to

$$v_0 = \left(\frac{2f}{\rho r}\right)^{1/2} \tag{16}$$

It is the time-dependent character of the capillary force that explains a qualitatively different behavior in the case of hydrophobic capillaries.

The prediction that, initially, the meniscus moves at a constant speed is supported by a series of measurements with aqueous solutions of $C_{14}E_6$ and $C_{10}E_6$ surfactants at different concentrations (Figs. 2 and 3). The same experiment shows that for these surfactants the initial delay does not exceed 1 s and apparently reduces with increasing surfactant concentration. Furthermore, experiments with different capillaries seem to support the conclusion that the initial velocity increases with increasing the capillary size (Fig. 6). However, this result is not quite conclusive because the degree of hydrophobization may to some extent vary from capillary to capillary.

Mathematical considerations. Summarizing the aforesaid, the following problem can be posed: find functions $z(t)$ and $c(\zeta, t)$ that satisfy the equation of dynamics,

$$\rho[zz'' + (z')^2] = \frac{2}{r}\,f(t) - \frac{8}{r^2}\,zz' - \rho gz \tag{17}$$

where ρ is the density, and η, the viscosity, of capillary liquid, and g is the acceleration of gravity, and the equation of diffusion,

$$\frac{\partial c}{\partial t} = D\,\frac{\partial^2 c}{\partial \zeta^2} - z'\,\frac{\partial c}{\partial \zeta} \quad (0 < \zeta < z) \tag{18}$$

under the following constraints

$$z(0) = 0 \tag{19}$$

$$z'(0) = \frac{rk_{ls}^{+}\,\Gamma_{lv}^{eq}}{h\Gamma_{ls}^{m}} \tag{20}$$

$$c(0, t) = c_b \tag{21}$$

$$c(z, t) = F^{-1} \circ \Gamma_{lv}(t) \tag{22}$$

$$\left.\frac{\partial c}{\partial \zeta}\right|_{\zeta=0} = -\frac{k_{ls}^{+}\,\Gamma_{lv}^{eq}}{hD} \tag{23}$$

$$\int_0^{z(t)} [c_b - c(\zeta, t) - \frac{2}{r}\,\Gamma_{ls}(\zeta)]\,\mathrm{d}\zeta = \varphi(t)\Gamma_{lv}(t) - \varphi(0)\Gamma_{lv}(0) \tag{24}$$

where $F(c)$ represents the adsorption isotherm and F^{-1} designates the inverse function. Eqn. (22) implies instant equilibration between the surface and subsurface at the lv interface (*i.e.* the adsorption from solution to the lv interface is a diffusion-controlled process). It is also evident that $\Gamma_{lv}(0) = F \circ c_b = \Gamma_{lv}^{eq}$. Modification for the case of mixed kinetics is rather straightforward and is not discussed here. The function $\varphi(t)$ takes into account the variation in the area of the lv interface with varying the contact angle,

$$\varphi(t) = \frac{2}{1 + |\cos\,\theta(t)|} \tag{25}$$

$$\cos\,\theta(t) = \frac{\gamma_{lv}(t) - [\gamma_{ls}^{180} - \gamma_{ls}^{0}]\exp\left(-\dfrac{k_{ls}^{+}\,\Gamma_{lv}(t)}{\Gamma_{ls}^{m}\,z'(t)}\right)}{\gamma_{lv}(t)} \tag{26}$$

It should be noted that eqn. (26) describes the contact angle dynamics under quasi-equilibrium conditions, when the contact angle is uniquely determined by the momentary force balance at the tcl. This condition can only be fulfilled when mechanical equilibration of the meniscus is much faster than the surface tension relaxation. For pure liquids and for sufficiently viscous solutions, this is not usually the case, and the contact angle dynamics is largely influenced by purely hydrodynamic effects.[11,30,31]

Finally,

$$f(t) = \gamma_{lv}(t)\left[1 - 2\,\exp\left(-\frac{k_{ls}^{+}\,\Gamma_{lv}(t)}{\Gamma_{ls}^{m}\,z'(t)}\right)\right] \tag{27}$$

and

$$\gamma_{lv}(t) = \gamma_{lv}^{0} - RT\int_{c=0}^{c=c(z,\,t)} \Gamma_{lv}(t)\,\mathrm{d}\,\ln\,c \tag{28}$$

according to the Gibbs equation. If adsorption at the lv interface is described by the Langmuir isotherm, then eqns. (22) and (28) are transformed into

$$c(z, t) = \frac{\Gamma_{lv}(t)}{K_{lv}^{L}[\Gamma_{lv}^{m} - \Gamma_{lv}(t)]} \tag{29}$$

and

$$\gamma_{lv}(t) = \gamma_{lv}^{0} + \Gamma_{lv}^{m}RT\,\ln\left[1 - \frac{\Gamma_{lv}(t)}{\Gamma_{lv}^{m}}\right] \tag{30}$$

respectively. Here K_{lv}^{L} is the Langmuir adsorption equilibrium constant and Γ_{lv}^{m} is the monolayer capacity for the lv interface (it does not differ much from Γ_{ls}^{m}).

Notice that in eqns. (17)–(30) the zero time has been redefined so that $f(0) = 0$, *i.e.* it is shifted by τ from the actual touching of the capillary to the liquid surface.

To enable use of the approximate eqn. (27) in place of the exact eqn. (9), one has to take $h = r\,\ln 2$. Since the final rise height is typically much larger than the capillary radius–rigorously speaking, this is one of the conditions justifying the neglect of the flow pattern effects in the head-zone near the entrance point in the equation of dynamics—this trick does not affect the final result significantly. In fact, it simply reflects the fact that the approximate relation $\int \Gamma_{lv}\,\mathrm{d}t \approx \Gamma_{lv}h/z'$ is no longer applicable once $z < r$.

Two limiting regimes of capillary rise dynamics

1. *Strong depletion near the lv interface* ($\Gamma_{lv} \ll \Gamma_{lv}^{eq}$). Simple estimates show that in most cases the extension of the diffusion zone is much less than z and scales as $(Dt)^{1/2}$ with time. Hence the concentration gradient is approximately proportional to $c_b/(Dt)^{1/2}$. Within certain time limits, the capillary rise represents a quasi-steady process, *viz.* the amount of surfactant adsorbed to the ls interface per unit time is equal to that brought to the lv interface by diffusion,

$$2\pi r\Gamma_{ls}^{m}\,\mathrm{d}z \approx \pi r^2 D\,\frac{c_b}{(Dt)^{1/2}}\,\mathrm{d}t. \tag{31}$$

which leads to the following scaling relation,

$$z(t) \approx \frac{rc_b}{\Gamma_{ls}^{m}}\,(Dt)^{1/2} \tag{32}$$

This explains the nearly linear appearance of the z *vs.* $t^{1/2}$ plots within certain time limits (Figs. 5 and 6). In this connec-

tion, it should be stressed that the Lucas–Washburn equation, which also predicts a linear proportionality between z and $t^{1/2}$ in the short-time limit, is not generally applicable to surfactant systems in which adsorption at the ls is important (*cf.* Figs. 2 and 3). It also fails to explain the existence of an induction period in the capillary rise dynamics (*cf.* eqn. (20)).

2. *Weak depletion near the lv interface* ($\Gamma_{lv} \approx \Gamma_{lv}^{eq}$). Two different scenarios can be proposed in this case: (i) a slow drift to the equilibrium level (Fig. 8) and (ii) an overshoot followed by relaxation to the equilibrium level (Figs. 9, 10 and 12).

The first scenario occurs when the adsorption at the ls interface equilibrates relatively slowly. First, z rises relatively rapidly to a quasi-equilibrium level that is slowly drifting due to relaxation of the adsorbed layer. To analyze the dynamics of this drift, differentiate the expression

$$z = \frac{2\gamma_{lv} \cos\theta}{\rho g r} \tag{33}$$

by time. This gives

$$\frac{dz}{dt} = \frac{2}{\rho g r}\left(\cos\theta \frac{d\gamma_{lv}}{dt} - \gamma_{lv} \sin\theta \frac{d\theta}{dt}\right) \tag{34}$$

For diffusion-controlled adsorption kinetics,

$$\frac{d\gamma_{lv}}{dt} = -\frac{\gamma_{lv}^{eq}}{2}\frac{\tau_D^{1/2}}{t^{3/2}} \tag{35}$$

where τ_D is defined by

$$\tau_D = \frac{\pi}{D}\left(\frac{RT}{2c_b\gamma_{lv}^{eq}}\right)^2 (\Gamma_{lv}^{eq})^4 \tag{36}$$

and can be regarded as the equilibration time for diffusion-controlled adsorption. It should be noted that, mathematically, the equilibrium state is never attained exactly – it is only approached asymptotically with a speed proportional to τ_D^{-1}. For $c_b \sim 10^{-3}$ mol dm^{-3}, $\gamma_{lv}^{eq} \sim 3 \times 10^{-2}$ N m^{-1}, $\Gamma_{lv}^{eq} \sim 4 \times 10^{-6}$ mol m^{-2}, $T \sim 300$ K, and $D \sim 10^{-9}$ m^2 s^{-1}, one gets $\tau_D \sim 10^{-3}$ s.

Further, one needs to evaluate $d\theta/dt$. From eqn. (26) it follows

$$\frac{d\theta}{dt} = \frac{\Delta\gamma_{ls}}{\sin\theta}\frac{d}{dt}\left[\frac{1}{\gamma_{lv}}\exp\left(-\frac{k_{ls}^+\Gamma_{lv}}{\Gamma_{ls}^m z'}\right)\right] \tag{37}$$

where $\Delta\gamma_{ls} = \gamma_{ls}^{180} - \gamma_{ls}^0$. After some arithmetic, one finds

$$\gamma_{lv}\sin\theta\frac{d\theta}{dt} = -\Delta\gamma_{ls}\exp\left(-\frac{k_{ls}^+\Gamma_{lv}}{\Gamma_{ls}^m z'}\right) \times\left[\frac{k_{ls}^+}{\Gamma_{ls}^m}\left(\frac{\Gamma_{lv}'}{z'} - \Gamma_{lv}\frac{z''}{(z')^2}\right) + \frac{\gamma_{lv}'}{\gamma_{lv}}\right] \tag{38}$$

An important conclusion is that as z' tends to zero, the latter term becomes negligible. Therefore, at the final stage, z' is always proportional to γ_{lv}' and has to decrease with time. However, if the adsorption equilibration time, τ_D, is much smaller than the capillary filling time,

$$\tau_F = \frac{16\eta\gamma_{lv}^{eq}\cos\theta^{eq}}{(\rho g)^2 r^3} \tag{39}$$

the resulting decrease is so small that it cannot be detected experimentally. Experiment will only show liquid rising to an equilibrium level, which then stays essentially the same except for small fluctuations in either direction. More interesting observations can be made if the capillary filling rate is limited by adsorption to the ls interface, *i.e.* if k_{ls}^+ is relatively small. As z is approaching a quasi-equilibrium level, a bend point has to be passed, where $|z''|$ is relatively large while z' is small. Under such circumstances,

$$\frac{dz}{dt} \approx -A\exp\left(-\frac{B}{z'}\right)\frac{z''}{(z')^2}; \quad A = \frac{2\Delta\gamma_{ls}}{\rho g r}B; \quad B = \frac{k_{ls}^+\Gamma_{lv}}{\Gamma_{ls}^m} \tag{40}$$

Changing to finite-difference representations, one finds

$$z_{n+1} = z_n + v_n\Delta t\left[1 - \frac{v_n^2}{A}\exp\left(\frac{B}{v_n}\right)\Delta t\right], \quad \Delta t = t_{n+1} - t_n \tag{41}$$

where $v = z'$ represents the velocity. Thus, z will keep increasing within certain time limits after a quasi-stationary level has been attained, decelerating with time. When the velocity gets small enough, the first term in eqn. (34) starts to dominate as noted before.

The second long-time scenario is a rather universal one involving an initial solution rise above its equilibrium level and then a decline back to this level, yet it can rarely be detected experimentally. For the overshoot to be large enough to make its detection possible, the capillary filling time, τ_F, has to be slightly less than the surface tension relaxation time, τ_D, the magnitude of the surface tension drop must be significant and the adsorption at the ls interface has to be fast. A concomitant relaxation of the ls interface may otherwise mask this effect. A formal mathematical proof follows: let γ_{lv} evolve according to the Ward–Tordai theory,

$$\gamma = \gamma_0 - RTK_H c_b[1 - \exp(at)\mathrm{erfc}(at)^{1/2}], \quad a = D/K_H^2 \tag{42}$$

where K_H is the Henry adsorption constant. In this case, $1/a$ can be thought of as a measure of the adsorption equilibration time (this definition is different from that given in eqn. (36)). Substituting eqn. (42) into eqn. (17), differentiating by time, and taking into account that the first derivative of z turns into zero in the maximum, $z'(t_m) = 0$, one gets

$$a\exp(at)\mathrm{erfc}(at)^{1/2} - \frac{1}{2}\left(\frac{a}{t}\right)^{1/2} = Czz'', \quad C = \frac{4\eta}{rRTK_H c_b} \tag{43}$$

Herewith, for the sake of simplicity, the solid surface was assumed to be completely wettable. As $t \to 0$, the left-hand side tends to $-\infty$ while the right-hand side tends to $+\infty$, and as $t \to \infty$, the left-hand side decays as $(a/t)^{1/2}$, while the right-hand side decays as $\exp(-t/\tau_F)$. For a maximum to exist (*i.e.* t_m to be finite), these two branches have to intersect, which is only possible if the product $a\tau_F$ does not exceed a certain limiting value.

Role of micelles. The presence of micelles in concentrated surfactant systems makes the transport processes more complex. For the same total concentration of surfactant in solution, longer alkyl chain surfactants are aggregated to a greater degree than shorter chain analogs. Micelles move more slowly than monomers and cannot directly adsorb to a hydrophobic surface. As a result, a solution of $C_{10}E_6$ surfactant rises significantly faster than a solution of $C_{14}E_6$ of the same concentration (Fig. 4). There exists dynamic exchange between the molecular and aggregated forms of surfactant. The decay of micelles replenishes the supply of monomers in the regions depleted of molecular surfactant by adsorption. As a result, the transport eqn. (18) has to be replaced by a system of equations, one for monomer, and another for micellar transport, coupled through a source function, Q, describing monomer–micelle exchange,

$$\frac{\partial c_1}{\partial t} = D_1\frac{\partial^2 c_1}{\partial\zeta^2} - z'\frac{\partial c_1}{\partial z} + Q(\zeta, t)$$

$$\frac{\partial c_N}{\partial t} = D_N\frac{\partial^2 c_N}{\partial\zeta^2} - z'\frac{\partial c_N}{\partial\zeta} - Q(\zeta, t) \tag{44}$$

$$(0 < \zeta < z)$$

Here c_1 and c_N are the concentration of monomers and micelles, respectively, and D_1 and D_N, are the corresponding diffu-

sion coefficients. The source function has the form

$$Q(\zeta, t) = [\text{c.m.c.} - c_1(\zeta, t)][k_1(t)c_N(\zeta, t) + k_N(t)c_1(\zeta, t)] \quad (45)$$

The kinetic parameters, k_1 and k_N, characterize the intensity of concurrent processes of disaggregation and aggregation of surfactant. For a more detailed discussion on the transport phenomena in concentrated surfactant solutions the reader is referred to our previous work.[24]

Conclusions

The flow behavior of complex surfactant solutions in cylindrical capillaries has been studied. In hydrophobic capillaries, three limiting kinetic regimes are identified. The initial rise is characterized by a linear dependence between the height, z, of the advancing meniscus and the time, t. At this stage, a quasi-steady process takes place, when the rise rate is limited by the adsorption of surfactant to the ls interface. This leads to a linear increase in the capillary force with time. During the initial rise period, the lv interface becomes depleted of surfactant and a diffusion zone is built up in the front of the rising liquid column. After some time, the capillary rise kinetics start to depend more and more on the surfactant mass transport in this expanding zone, finally leading to $z \sim t^{1/2}$. This is the second kinetic regime. The characteristic dynamic behavior in the third kinetic regime, referred to as the long-time relaxation regime, is a very slow meniscus height drift towards the equilibrium height. This slow drift is believed to be caused by the surface tension relaxation at the lv interface and adsorption equalization across the ls interface.

High c.m.c. surfactants, *e.g.* $C_{10}E_6$, rise much faster than the low c.m.c. surfactants, *e.g.* $C_{14}E_6$. The main origin of this strong dependence, also seen in the surface tension relaxation rates, is slower diffusivity of surfactants in the micellar state as compared to the monomer state, although some difference in micelle dissociation rates can play a certain role as well. Variations in micelle size and adsorption rate constants also influence the flow dynamics. These effects can be analyzed in the framework of the presented theoretical model.

In hydrophilic capillaries, the dynamics in the initial part of the rise is reminiscent of that for pure water. Both systems exhibit an initial $z \sim t^{1/2}$ dependence of the capillary rise. For the surfactant solutions, the initial rate can be affected by the reduction of the lv tension. This effect is significant if the lv interface has been allowed to relax before contact between the solution surface and the capillary is established. For solutions with freshly formed lv interfaces, the initial rate is similar to that observed for water. In this situation, an overshoot of the rise can be observed, which is followed by a damping to the equilibrium level as the lv tension relaxes.

Acknowledgements

This work was performed in the framework of the Paper Surfaces for Digital Printing Program supported by the Swedish Foundation for Strategic Research. Partial financing by the Swedish Pulp and Paper Research Foundation is also acknowledged.

References

1 G. Hagen, *Ann. Phys. Chem.*, 1839, **46**, 423.
2 J. L. Poiseuille, *C.R. Acad. Sci. Paris*, 1840, **11**, 961.
3 J. L. Poiseuille, *C.R. Acad. Sci. Paris*, 1841, **12**, 112.
4 R. Lucas, *Kolloid Z*, 1918, **23**, 15.
5 E. W. Washburn, *Phys. Rev.*, 1921, **17**, 273.
6 E. K. Rideal, *Philos. Mag. Ser. 6*, 1922, **44**, 1152.
7 C. H. Bosanquet, *Philos. Mag. Ser. 6*, 1923, **45**, 525.
8 F. P. Buff, *The Theory of Capillarity*, in *The Handbook of Experimental Physics*, ed. S. Flügge, Springer, Berlin, 1960, vol. 10.
9 J. Szekely, A. W. Neumann and Y. K. Chuang, *J. Colloid Interface Sci.*, 1971, **35**, 273.
10 S. Levine and G. H. Neale, *J. Chem. Soc., Faraday Trans. 2*, 1975, **71**, 12.
11 S. Levine, J. Lowdnes, E. J. Watson and G. Neale, *J. Colloid Interface Sci.*, 1980, **73**, 136.
12 V. V. Krotov and A. I. Rusanov, *Physicochemical Hydrodynamics of Capillary Systems*, Imperial College Press, London, 1999.
13 D. Quére, E. Raphael and J.-Y. Ollitrault, *Langmuir*, 1999, **15**, 3679.
14 B. V. Zhmud, F. T. Tiberg and K. Hallstensson, *J. Colloid Interface Sci.*, 2000, **228**, 263.
15 J. R. Ligenza and R. B. Bernstein, *J. Am. Chem. Soc.*, 1951, **73**, 4636.
16 L. R. Fisher and P. D. Lark, *J. Colloid Interface Sci.*, 1979, **69**, 486.
17 R. S. Malik, C. H. Larouissi and L. W. de Becker, *Soil Sci.*, 1979, **127**, 211.
18 K. T. Hodgson and J. C. Berg, *J. Colloid Interface Sci.*, 1988, **121**, 22.
19 S. Padmanabhan and A. Bose, *J. Colloid Interface Sci.*, 1988, **126**, 164.
20 N. V. Churaev and Z. M. Zorin, *Colloids Surf. A*, 1995, **100**, 131.
21 N. V. Churaev, A. P. Ershov and Z. M. Zorin, *J. Colloid Interface Sci.*, 1996, **177**, 589.
22 V. V. Krotov and A. I. Rusanov, *Kolloidn. Zh.*, 1977, **39**, 48.
23 V. B. Fainerman, *Kolloidn. Zh.*, 1981, **43**, 94.
24 B. V. Zhmud, F. Tiberg and J. Kizling, *Langmuir*, 2000, **16**, 2557.
25 F. M. Folkes, *J. Phys. Chem.*, 1953, **57**, 98.
26 R. M. Hill, M. He, H. T. Davis and L. E. Scriven, *Langmuir*, 1994, **10**, 1724.
27 R. M. Hill, *Curr. Opin. Colloid Interface Sci.*, 1998, **3**, 247.
28 T. Stoebe, Z. Lin, R. M. Hill, M. D. Ward and H. T. Davis, *Langmuir*, 1996, **12**, 337.
29 J. Eriksson and F. Tiberg, work in preparation.
30 P. G. de Gennes, *Rev. Mol. Phys.*, 1985, **57**, 827.
31 E. B. Dussan, *Ann. Rev. Fluid Mech.*, 1979, **11**, 371.